



LAWRENCE  
LIVERMORE  
NATIONAL  
LABORATORY

# Microscopic Calculation of Fission Fragment Energies for the $^{239}\text{Pu}(n, f)$ Reaction

W. Younes, D. Gogny

October 4, 2011

## **Disclaimer**

---

This document was prepared as an account of work sponsored by an agency of the United States government. Neither the United States government nor Lawrence Livermore National Security, LLC, nor any of their employees makes any warranty, expressed or implied, or assumes any legal liability or responsibility for the accuracy, completeness, or usefulness of any information, apparatus, product, or process disclosed, or represents that its use would not infringe privately owned rights. Reference herein to any specific commercial product, process, or service by trade name, trademark, manufacturer, or otherwise does not necessarily constitute or imply its endorsement, recommendation, or favoring by the United States government or Lawrence Livermore National Security, LLC. The views and opinions of authors expressed herein do not necessarily state or reflect those of the United States government or Lawrence Livermore National Security, LLC, and shall not be used for advertising or product endorsement purposes.

This work performed under the auspices of the U.S. Department of Energy by Lawrence Livermore National Laboratory under Contract DE-AC52-07NA27344.

# Microscopic calculation of fission fragment energies for the

## $^{239}\text{Pu}(n_{th}, f)$ reaction

W. Younes and D. Gogny

*Lawrence Livermore National Laboratory, Livermore CA 94551*

(Dated: October 3, 2011)

### Abstract

We calculate the total kinetic and excitation energies of fragments produced in the thermal-induced fission of  $^{239}\text{Pu}$ . This result is a proof-of-principle demonstration for a microscopic approach to the calculation of fission-fragment observables for applied data needs. In addition, the calculations highlight the application of a fully quantum mechanical description of scission, and the importance of exploring scission configurations as a function of the moments of the fragments, rather than through global constraints on the moments of the fissioning nucleus.

## I. INTRODUCTION

An effort is underway at LLNL to develop a microscopic framework which, starting from protons, neutrons, and an effective interaction between them, uses the methods of many-body physics to move toward a predictive and comprehensive theory of nuclear fission. In the first phase of this project, we attempt to extract realistic properties of the fission fragments—e.g., kinetic and excitation energies, shapes, yields—for neutron-induced fission on a  $^{239}\text{Pu}$  target from thermal to 14-MeV incident energies. The appeal of a microscopic approach to fission is twofold. First, the only phenomenological input to the theory is the effective interaction between nucleons, with all other aspects of the theory deduced from the laws of quantum mechanics. Since that interaction is the same regardless of the nucleus, its shape, its energy, and even the specific phenomenon being studied (see, e.g., [1]) the microscopic approach is a good candidate for a predictive theory of fission. Second, the output from the theory is a time-dependent wave function describing the fissioning nucleus, from which all observables can in principle be rigorously extracted. Thus, the microscopic approach is a good candidate for a comprehensive theory of fission.

In this report, we present proof-of-principle calculations of the kinetic and excitation energies of the fragments at scission, for the  $^{239}\text{Pu}(n_{th}, f)$  reaction. The main result is given in Fig. 1. These fragment properties are a critical input to the phenomenological code FREYA [2], which tracks the fragments and their emitted neutrons and gammas beyond scission, and produces observables such as the fission-neutron spectrum that can be directly compared to experiment.

## II. THEORY

In this report we only present results of static calculations of the nuclear configurations near and at scission. Dynamical calculations of the evolution in time of the nucleus toward these scission configurations will be performed in subsequent work, and will essentially give a population probability for each of these scission configurations. Examples of such dynamical calculations can be found in [3, 4]. The relevant nuclear configurations were calculated using the LLNL-developed Hartree-Fock-Bogoliubov code FRANCHBRIE [5], and the settings used for the calculations can be found in [6].

As in [6], we explored configurations of the fissioning  $^{240}\text{Pu}$  nucleus described through constraints on its collective quadrupole ( $Q_{20}$ ) and octupole ( $Q_{30}$ ) moments, as well as the size of the neck ( $Q_N$ ) connecting the pre-fragments. Those configurations corresponding to scission were identified, and the associated fragment properties were extracted using a quantum mechanical approach described in [7]. Thus a large set of scission configurations was obtained, spanning heavy-fragment masses ( $A_H$ ) between 120 and 164 and the full spectrum of fission modes from hot (maximally excited fragments) to cold (little or no fragment excitation).

In addition to the calculations using global constraints on the  $Q_{20}$ ,  $Q_{30}$ , and  $Q_N$  degrees of freedom, we have also performed a set of calculations with constraints on the properties of the individual fragments (i.e., their numbers of protons and neutrons and their quadrupole moments) and the separation distance between them. These calculations were motivated by the observed paucity of configurations that could be obtained for  $A_H \gtrsim 134$  with global constraints alone. Furthermore, it is to be expected that, as one nears scission and the nucleus begins to divide into two pre-fragments, constraints on those individual pre-fragments should provide a richer and more accurate description of the fission phenomenon than the global constraints. The calculations with individual fragment constraints were only performed for the range  $A_H = 134 - 160$  due to limitations in computational resources. To the best of our knowledge, this is the first time in the literature that local constraints on the fragments themselves have been used to describe fission.

Finally, because the present calculations are static and adiabatic (i.e., they do not account for the possibility of exciting non-collective states of the  $^{240}\text{Pu}$  nucleus on the way to scission), they do not therefore explicitly account for the partition of the energy acquired in the descent from saddle to scission into kinetic and excitation energy of the fragments. The inclusion of non-adiabatic effects within a microscopic theory is in progress [8], but for the present work we adopt the simple model discussed in [7], wherein half of the available energy contributes to the total excitation energy (TXE) of the fragments, and the other half contributes to their total kinetic energy (TKE). There is some basis, as discussed in [7], to presume that this simple picture of non-adiabatic effects is not too far from the mark.

### III. RESULTS

The calculated TXE and TKE are shown in Fig. 1 and compared to experimental data. The TKE is plotted in the top panel as a function of the heavy-fragment mass. The TKE data are taken from [9–11], and the one-sigma values about the experimental average TKE values are taken from [12]. Calculations with both global and local (fragment) constraints are shown. Similarly, in the bottom panel we show the TXE as a function of heavy-fragment mass. A line representing the empirical “maximum” TXE is taken from [13], and was estimated from the binding energies of the fragments, the average number of neutrons they emit and their average kinetic energies, and the energy emitted by gamma decay (estimated as one half the binding energy of the first neutron not emitted). Therefore, because of the assumptions and approximations used in its calculation, the empirical line is not to be taken as the true maximum energy, but more as a guide. Here again, calculations with both global and local (fragment) constraints are shown.

Given that these are microscopic calculations starting from an effective interaction and not a fit to fission data, the level of agreement between data and calculation for both TKE and TXE is somewhat remarkable. To be sure, that agreement is not perfect, especially for the locally constrained calculations where hot-fission points appear to give TKE (TXE) values that are a bit too low (high). However, it is important to keep in mind that these are static results. Dynamic calculations will provide a weight for each calculated point in Fig. 1, and it remains to be seen whether the apparent outliers are significantly populated during fission. In any case, Fig. 1 clearly shows the importance of local constraints near scission, since many of the points on the figure could not be obtained with global constraints alone.

### IV. CONCLUSION

Using a static microscopic calculation of configurations at and near scission, we have identified fission fragments for the  $^{239}\text{Pu}(n_{th}, f)$  reaction and extracted their total kinetic and excitation energies. Comparison with data shows very good overall agreement between theory and experiment. Beyond their success as a proof of principle, these calculations also highlight the importance of local constraints on the fragments themselves in microscopic calculations. In the future, we will improve on the current results in the following ways:

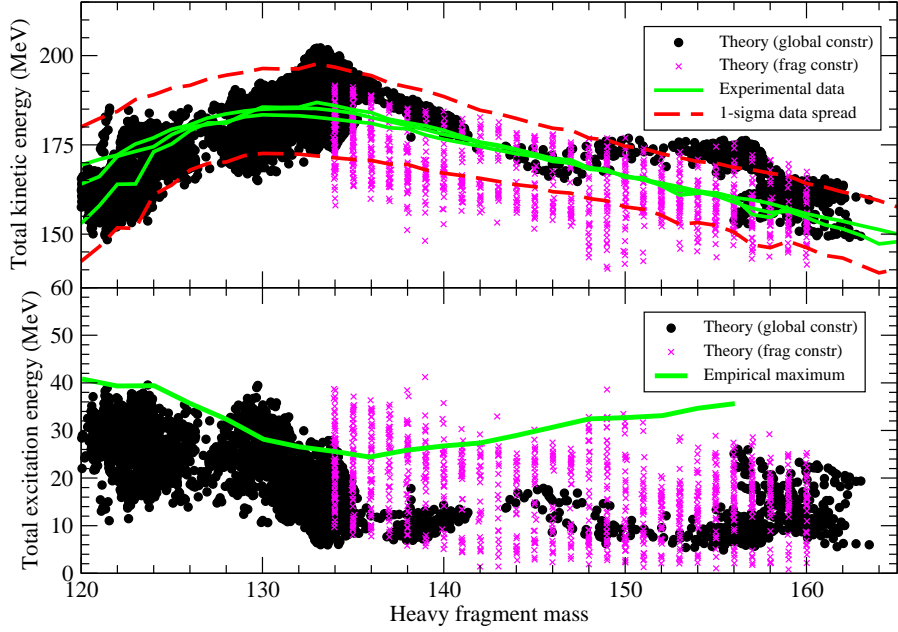


Figure 1: Comparison of calculated and experimental TKE (top panel) and TXE (bottom panel) for the  $^{239}\text{Pu}(n_{th}, f)$  reaction. Microscopic theory calculations are shown with both global and local (fragment) constraints. See text for additional details.

1) we will perform a more comprehensive set of calculations for  $A_H = 120 - 160$  with the local fragment constraints, 2) we will perform dynamical calculations of fission to associate a population probability with each scission configuration, 3) we will study the effect of non-adiabatic motion within a more microscopic framework to better understand the partition of the saddle-to-scission energy into kinetic and excitation energy of the fragments, 4) we will perform a similar calculation of TKE and TXE for the  $^{235}\text{U}(n_{th}, f)$  reaction as an additional benchmark, and 5) we will extend the approach described in this report to higher-energy fission and calculate fragment properties for up to 14-MeV incident neutron energies in the  $^{239}\text{Pu}(n, f)$  reaction.

## Acknowledgments

This work was performed under the auspices of the US Department of Energy by the Lawrence Livermore National Laboratory under Contract DE-AC52-07NA27344.

---

- [1] J.-P. Delaroche, M. Girod, J. Libert, H. Goutte, S. Hilaire, S. Péru, N. Pillet, and G. F. Bertsch, *Phys. Rev. C* **81**, 014303 (2010).
- [2] J. Randrup and R. Vogt, *Phys. Rev. C* **80**, 024601 (2009).
- [3] J.-F. Berger, M. Girod, and D. Gogny, *Nucl. Phys.* **A502**, 85 (1989).
- [4] H. Goutte, J.-F. Berger, P. Casoli, and D. Gogny, *Phys. Rev. C* **71**, 024316 (2005).
- [5] W. Younes and D. Gogny, LLNL Tech. Rep. UCRL-TR-234682, 2007 (unpublished).
- [6] W. Younes and D. Gogny, *Phys. Rev. C* **80**, 054313 (2009).
- [7] W. Younes and D. Gogny, *Phys. Rev. Lett.* **107**, 132501 (2011).
- [8] R. Bernard, H. Goutte, D. Gogny, and W. Younes, [*Phys. Rev. C* (to be published)].
- [9] C. Wagemans, E. Allaert, A. Deruytter, R. Barthélémy, and P. Schillebeeckx, *Phys. Rev. C* **30**, 218 (1984).
- [10] K. Nishio, Y. Nakagome, I. Kanno, and I. Kimura, *J. Nucl. Sci. Technol.* **32**, 404 (1995).
- [11] C. Tsuchiya, Y. Nakagome, H. Yamana, H. Moriyama, K. Nishio, I. Kanno, K. Shin, and I. Kimura, *J. Nucl. Sci. Technol.* **37**, 941 (2000).
- [12] M. Asghar, F. Cañucoli, P. Perrin, and C. Wagemans, *Nucl. Phys.* **A311**, 205 (1978).
- [13] J. Neiler, F. J. Walter, and H. W. Schmitt, *Phys. Rev.* **149**, 894 (1966).